Determination of Aflatoxin B1-induced cancer stem cells using 3D bioprinting

3D 바이오프린팅을 이용한 Aflatoxin B1-유도 암 줄기세포의 측정

February 2023

Cao Viet Phuong

Determination of Aflatoxin B1−induced cancer stem cells using 3D bioprinting

Under the guidance of Professor Joon Myong Song

Submitting a master's thesis of pharmacy

January 2023

Graduate School of Pharmacy
Seoul National University
Pharmaceutical Science Major

Cao Viet Phuong

Confirming the master's thesis written by
Cao Viet Phuong
February 2023

Chair	Kwon, Sung Won
Vice Chair	Kang, Yun Pyo
Examiner	Song, Joon Myong

Abstract

Aflatoxin B1 is a mycotoxin derived from fungus species *Aspergillus flavus* and *Aspergillus parasiticus*, whose carcinogenicity is widely known. However, its involvement in cancer stem cell induction remains vague, which has been observed in 2D cell culture model only. However, due to limitations of 2D cell culture and its disparity with *in vivo* condition, a clinically more relevant observation should be established. This study develops a 3D cell culture facilitated by 3D bioprinting to examine the hypothesis about whether Aflatoxin-B1 exposure enhances cancer stem cell population on HepG2 liver cancer cell line. Following a 7-day spheroid growth and 48-hour Aflatoxin-B1 treatment, two biomarkers, CD133, or prominin-1, and Aldehyde dehydrogenase 1 (ALDH1), are employed to isolate cancer stem cells from the spheroids. The spheroids are analysed using 2 methods: confocal imaging shows a visible positivity of both markers, whereas fluorescence-activated cell sorting (FACS) offers a quantitative result about the percentages cancer stem cells occupied the entire population. Results from both methods demonstrate that cancer stem cell proportion increased when Aflatoxin-B1 concentration was elevated. On the one hand, the increment obtained from more than one method highlights a correlation between Aflatoxin-B1 exposure and cancer stem cell formation; on the other hand, similarity between two analysing methods suggested that besides the casual techniques related to flow cytometry, confocal imaging can offer a reliable finding about cancer stem cell analysis while do not disturbing the natural morphology of tumours.

Keywords: Aflatoxin B1, Cancer stem cells, 3D bioprinting, Liver spheroid.

List of Contents

List of Figures

List of Tables

List of abbreviations

CSC: cancer stem cell

ECM: extracellular matrix

FACS: fluorescence-activated cell sorting.

I. INTRODUCTION

1. Cancer stem cells

Cancer stem cells (CSCs) are defined as a minor cell population in a tumour that can asymmetrically divide to self-renew, as well as differentiate into various cell subtypes; furthermore, their transplantation into a new host also sustains new tumour growth (1). With respect to clinical relevance, due to multiple mechanisms, such as elevated DNA repair (2), enhanced autophagy (3),(4), or reduced ferrotopsis (5), CSCs have also been identified to be responsible for tumours' resistance to chemotherapies and radiotherapies, leading to cancer treatment failures and cancer recurrence. As a result, this makes them become a deeply-studied topic in cancer research over the past few years.

Stem-like characteristics of CSCs are preserved and displayed by an array of markers, which are molecules abnormally expressed because of modification in gene regulations. Additionally, since they uniquely appear in CSCs rather than normal cancer cells, and each cancer cell line is represented by a certain set of markers, the utilisation of these markers has been applicable to distinguish and isolate CSCs from the entire population of various cancer cell lines (6),(7),(8),(9).   .

2. Aflatoxin B1 as a carcinogen

Aflatoxin B1 is a mycotoxin stemming from *Aspergillus flavus* and *Aspergillus parasiticus*, which is widely known for its carcinogenicity due to inducing a mutation in p53 gene. Specifically, its metabolite by cytochrome P450 enzyme, exo-Aflatoxin B1-8,9-epoxide, can link with guanine and generate an adducts with DNA, the interfere of which with normal DNA structure can inhibit tumour

suppressor genes; as a result, cell growth is no longer properly control, so cancer is initiated (10).

Previously, while the correlation between Aflatoxin B1 and liver cancer pathogenesis is proved, its ability to induce CSCs in liver cancer cell line has been studied in 2D cell culture model (11).

3. 3D cell culture using bioprinting

However, a number drawbacks of 2D cell culture have been highlighted. For example, Birgersdotter et al. (12) indicated that in 2D cell culture, there is a lost in cell polarity, a pivotal feature of tissue, as well as an alteration in gene expression. Moreover, it also fails to preserve cells' natural morphology, and displaying a similarity in the accessibility of cells to media and drug solutions, as observed in *in vivo*. This explains a significant difference between results of *in vitro* studies using 2D cell culture and *in vivo* studies.

By contrast, 3D cell culture has been proved to better simulate physiological condition, especially tumour microenvironment. Indeed, since 3D-cultured cells grow in spheroid structure, they can maintain the nature shape while forming a tumour-like cluster with inner and outer layers, in which oxygen, nutrient and drug gradients emerge and make them less accessible to cells from inner layers (13). Additionally, by allowing the cells to grow in a gel-like structure, 3D cell culture also mimics extracellular matrix (ECM) (14). Therefore, results obtained in 3D cell culture model have been observed to be more resemble to *in vivo* context, reflected by aspects like higher cell viability (15) or more active drug metabolism (16), compared to 2D culture.

So far, a number of 3D cell culture techniques have been developed, and can be classified into scaffold-based and scaffold-free approach (17). Regarding scaffold-free models, although techniques are inexpensive and not labour-intensive, they enormously rely on the cell self-assemble; hence, they pose a challenge of producing a uniform spheroid size and shape, and these characteristics may significantly vary between distinct attempts. Meanwhile, in scaffold-based models, which are established using hydrogel, single cells are distributed in a fixed framework, so size and appearance control are more favourable, whereas its porous structure after cross-linking enables the hydrogel to serve as an artificial ECM, in which nutrients and soluble factors can be stored. In addition, when the hydrogel suspension entrapping cells are allocated into consistent polymer frame with similar amounts by 3D bioprinting, this can remarkably enhance reproducibility, so that variation between experiments can be reduced.

With the aforementioned background, the present study employed scaffold-based 3D cell culture facilitate by 3D bioprinting of hydrogel into a polymer structure to develop a model for examining the capability of Aflatoxin-B1 to induce cancer stem cell on HepG2 liver cancer cell line.
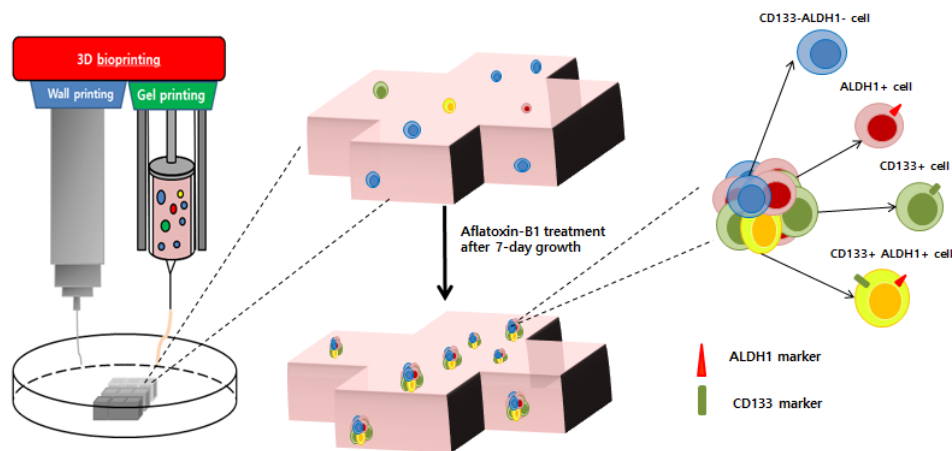
Figure 1. Schematic abstract.

3

II. METHODS

1. Cell culture

Liver cancer cell line HepG2 from Korea Cell line bank (NO.30022; Seoul, Korea) is employed for the experiment by culturing in Dulbecco's modified Eagle's medium (DMEM; Gibco, Grand Island, NY, USA) supplemented with 10% FBS (Gibco) and 1% antibiotic-antimycotic (Gibco) at 37 ℃ under 5% CO2. To maintain cell growth, media exchange is conducted every 48 hours after washing with Phosphate-buffered saline (1xPBS, pH 7.2; Gendepot, USA). When subculture is needed, the cells are washed with 1xPBS before detachment by trypsin (TrypLE Express; Gibco, Denmark) in 5 minutes.

2. Material preparation for 3D bioprinting

To mimic the extracellular matrix in tumor microenvironment, Gelatine and Alginate are employed and purchased in lyophilized powder form. Before the experiment, they are dispersed into 1xPBS at a concentration of 10% and 4% (m/v), respectively. The mixtures are heated up to 80℃ in 7 hours, during which they are mixed every single hour to give a homogenous gel, before keeping in 37℃. Finally, approximately 2.5 million HepG2 cells, prepared in 0.5ml of DMEM supplemented with 10% FBS and 1% antibiotic-antimycotic, is added and mixed gently with the gel, which can be immediately applied to cell 3D printing.

3. 3D bioprinting of mini-well

CAD program Rhino 6 is applied to design 3D mini well structure, which is subsequently converted into stl files to be applicable to New Creator K V1.57.70 software. Once the file is uploaded and the 3D printer is connected to the software, the fabrication of mini-well is initiated automatically. Briefly, thermoplastic poly

lactic acid (PLA) polymer is transformed into semisolid form by heating to 210℃, which flows through the nozzle as semisolid fiber with a size of 0.2 mm. By optimizing the filling density and printing speed at 75% and 10 mm/s, respectively, layer-by-layer printing is facilitated to form a mini-well which is 4mm high and covers an area of 14x14 mm. Each mini-well dish includes 9 wells arranged in a 3x3 square, and an individual well has a size of 3x3 mm.

4. 3D bioprinting of cell solution in hydrogel

 3D bioprinting of cell in hydrogel is conducted using the same 3D bioprinter and computer software with the previous step. In particular, the prepared hydrogel and cell mixture in previous step is loaded into a 10ml syringe and fixed in the dispenser of 3D bioprinter. Another stl file encoding the specialised design for gel printing is uploaded to the computer, which is already connected to the printer. Once printing commander is activated, the printer will automatically print the cell in gel mixture as cross-shaped structures into all 9 individual wells of the plate obtained from the previous step. When the wells are completely printed, the gel remains in semisolid state and need to be cross-linked by 160nM Calcium Chloride solution in DDW, which takes place in 10 minutes. The 3D-printed cells are maintained at 37°C and 5% CO_2, with nutrients provided by DMEM supplemented with 10% FBS and 1% antibiotic-antimycotic, which is exchanged every 24 hours. Their growths are monitored under the brightfield function of fluorescence microscope (Olympus BX51, Japan), where diameter measurement is possible.

5. Aflatoxin-B1 treatment

Aflatoxin-B1 was purchased as powder in 5mg vial (Enzo, Farmingdale, NY, USA). It is dissolved in DMSO to give the stock solution with a concentration of 0.5mg/ml, which is then kept at -20°C. For treatment to cell spheroids, this stock solution is diluted in serum-free DMEM media to 3 concentrations of 1µM, 2.5µM and 5µM.

After a 7-day growth of cell spheroids, DMEM supplemented with 10% FBS and 1% antibiotic-antimycotic is discarded and the gel structures are washed 2 times with 1xPBS. Subsequently, different plates are added with different solutions of 3 aforementioned concentrations of Aflatoxin-B1, along with the control, which contains only serum-free DMEM media. The carcinogen incubation takes place in 48 hours and is maintained at 37°C and 5% CO_2.

6. Immunostaining for surface marker detection on cell spheroids

In HepG2 liver cancer cell line, it displays the positivity of two important markers: CD133, or prominin-1, a transmembrane glycoprotein which has been widely selected to sort out liver cancer stem cells [18],[19],[20]; and ALDH1, a cytosolic enzyme responsible for intracellular retinoic acid formation [21]. Due to their significant role, this study employs these two markers to isolate cancer stem cells from the spheroids. Cell spheroids after exposure to Aflatoxin B1 at 4 different concentrations are washed 3 times with 1xPBS. Subsequently, fixation is conducted by adding 4% paraformaldehyde (PFA) at 4°C to the samples, which last for 20 minutes and is followed by a 3-time washing with PBS. In the next step, permeabilisation and blocking are made possible by immersing the samples into a

solution containing 0.2% Triton-X and 1% FBS in 1xPBS for 15 minutes. Following this, the samples are stained in 1 hour with Anti Alexa fluor 594 CD133 and Anti Alexa fluor 647 ALDH1 antibody solutions, at a dilution rate of 1:200, after which they are washed three times with 1xPBS. Finally, counter-staining is required, using Hoechst 33258 (Bloomington, MN 55431) at a dilution rate of 1:500 in 5 minutes, followed by a three-time wash using PBS. The samples are made available for imaging using confocal microscope (TCS SP8, Leica, Wetzlar, Germany) and LASX software after 3 times washing with 1xPBS. The obtained images are analysed with Imaris software (Bitplane, Zurich, Switzerland), while the fluorescence intensity is measured by Metamorph software (Molecular Devices, San Jose, CA, USA).

7. Quantification analysis with fluorescence-activated cell sorting (FACS)

Initially, cells spheroids are arranged randomly and maintained in a gel structure. To dissociate the gel, 500mg of Collagenase NB 4G Proved Grade powder is dispersed in 5ml DDW to form a solution, which is then added to the sample. By incubating the samples in 30 minutes at 37℃, the gel structure is totally dissociated. The broken and dissolved gels, along with remaining spheroids are collected and centrifuge at 1500rpm for 1 minute, and the supernatant is removed. The residue is dispersed in accutase and incubated in 37℃ for 10 minutes, after which spheroids are totally disintegrated into single cells. These single cells are fixed with 4% paraformaldehyde at 4℃ in 10 minutes. After fixation and discarding PFA, the samples are washed 2 times by dispersing in PBS, centrifuging and discarding the supernatant. Subsequently, cells are permeabilised and blocked with a mixture of 0.2% triton-X and 1%FBS prepared in PBS, which takes place in 10 minutes. In the next step, Anti alexa fluor 594 CD133 and Anti alexa fluor 647

ALDH1 antibodies are diluted in a buffer, which is originally 1% FBS solution in PBS, at a rate of 1:100, and applied to the sample for 1 hour. Finally, the antibody solution is discarded, before the sample is washed with PBS, dispersed in buffer, and applied to BD flow cytometer for quantification analysis.

III. RESULTS

1. The development of cell spheroid in hydrogel structure

To determine whether the bioprinting approach can facilitate a proper spheroid formation, the diameters of the spheroids was measured over a 7-day period using a bright-field microscope, in which images of the same area were taken every 24 hours. Figure 1 show the growth of cell spheroids and related measurement. As displayed by figure 1b, an increase in mean spheroid diameter is visible, in which the number started at an initial value of 18.5 μm and hit the peak of 39.2 μm on day 7, corresponding to a relative growth of more than 210%. The growth rate was maintained quite steadily throughout the period, despite a slight decrease from day 4 to day 5. In addition, it is observed that in terms of individual spheroids, there was a fluctuation in their attributions. Specifically, at the beginning, in comparison to the biggest single cells, whose diameter was around 25.5 μm, that of the smallest one was about 2 times lower, with only 13.1 μm (figure 1c). A similar variation was also observed on day 7, where the spheroid diameter ranged from 27.18 μm to 53.67 μm (figure 1d). Meanwhile, regarding individual spheroids, how much they grew also reflect an inconsistence. In particular, as reflected by figure 1D, spheroid number 18 grows the most significantly by more than 220%, whereas the least growing spheroid, numbered 12, grows by only 42%. The big growth rate of the former indicates that nutrients and oxygen were supplied properly, so a moderate growth of the latter can be attributed to its own biochemistry, rather than the downsides of the hydrogel structure. This result suggests that the developed 3D bioprinting model is an appropriate platform for 3D cell culture, which enables the cells to grow naturally, and hereby preserve the heterogeneity of the cell

population.
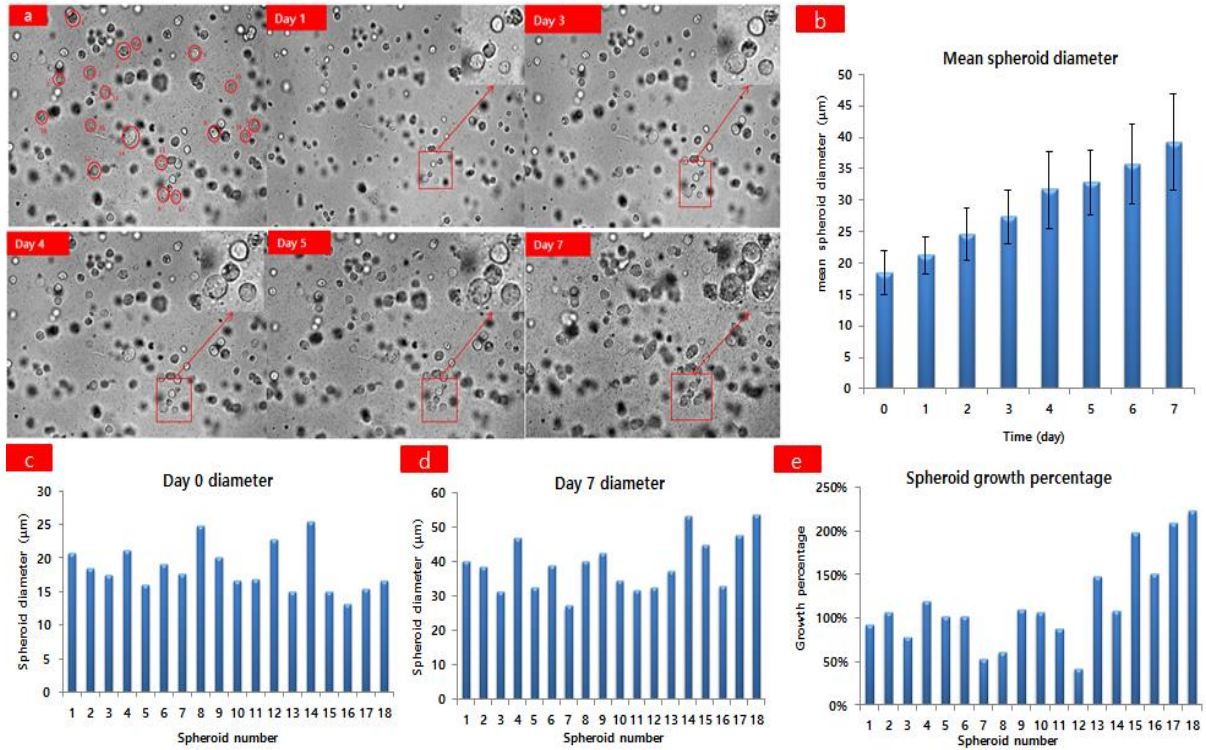
Figure 2. Daily measurement of cell spheroid. (a) Numbered spheroid and brightfield images of the same region throughout a 7-day period; (b) mean spheroid diameter throughout the period; (c) spheroid diameter measured on day 0 (immediately after printing); (d) spheroid diameter measured on day 7; (e) growth percentage of all numbered spheroid. .

2. Analysis of cancer stem cell marker expression by confocal imaging

Figure 2 demonstrates immunostaining results of HepG2 spheroids exposed to 4 different Aflatoxin-B1 concentrations, 0 μM, 1 μM, 2.5 μM, and 5 μM. The blue, green, and red signals indicate cell nuclear, CD133 and ALDH1 markers, respectively. In all images, the positivity of both CD133 and ALDH1 markers on HepG2 cell spheroids was clearly shown, and the extents to which they are expressed vary by concentration. In fact, among these markers, CD133 is expressed on cell surface, while ALDH1 exists in cytosol. Therefore, in cells where both markers are ideally found, an absolute overlap of these two markers cannot be detected; instead, CD133 signal surrounds that of ALDH1. As revealed

10

by the images, at the control, fluorescence intensity was shown in a small region of the spheroid, while at the highest concentration, the fluorescent region was expanded to the major region of the spheroid. In detail, the average fluorescence intensity measured over the whole spheroid surface, which is proportional to the expression level of each individual marker, increased gradually from the control to the 5 μM sample. Specifically, in comparison to the control, whose average intensities of CD133 and ALDH1 are 11.7 and 12.5, respectively, those of 5 μM gained by about 3 times, reaching 30.9, and 38.6, correspondingly (figure 2e). The increment reveals that the expression levels of each marker were enhanced as a result of Aflatoxin-B1 treatment.

Confocal imaging also enables an observation in single cell level. In specific, as cancer stem cells in present study are defined as cells expressing both CD133 and ALDH1, on imaging data, they display both green and red signal, corresponding to CD133 and ALDH1, respectively. In other words, cells with yellow signal, as a combination of green and red, are spotted as cancer stem cells. Figure 3a indicates the spheroid with spotted dots representing nuclear of single cells, in which grey dots represent non-cancer stem cells, whereas yellow dots represent cancer stem cells. By counting cancer stem cells and determining their proportion over the total cell numbers, the correlation between relative amount of cancer stem cells and Aflatoxin-B1 treatment can be established. As revealed by figure 3b, in control sample, the average CSC rate is approximately 6.6%, which increases by two times to 11.9% at 1 μM. The percentage increases gradually when Aflatoxin-B1 concentration gains, reaching the highest number of 31% at 5 μM. This result offers a clearer insight about the effect of Aflatoxin-B1 on cancer stem cell induction, in which cancer stem cells are observed in a more detailed level, and the increase of cancer stem cells has been firmly observed.
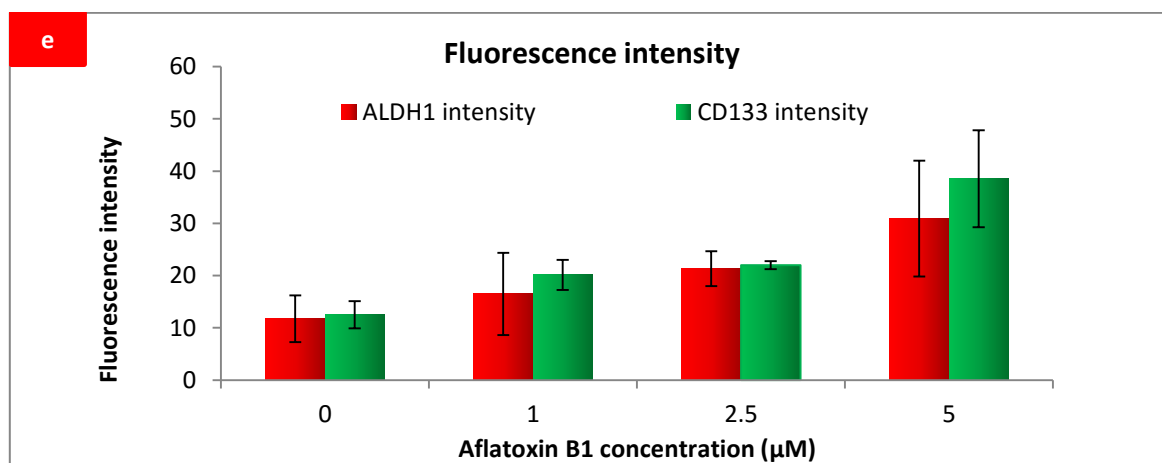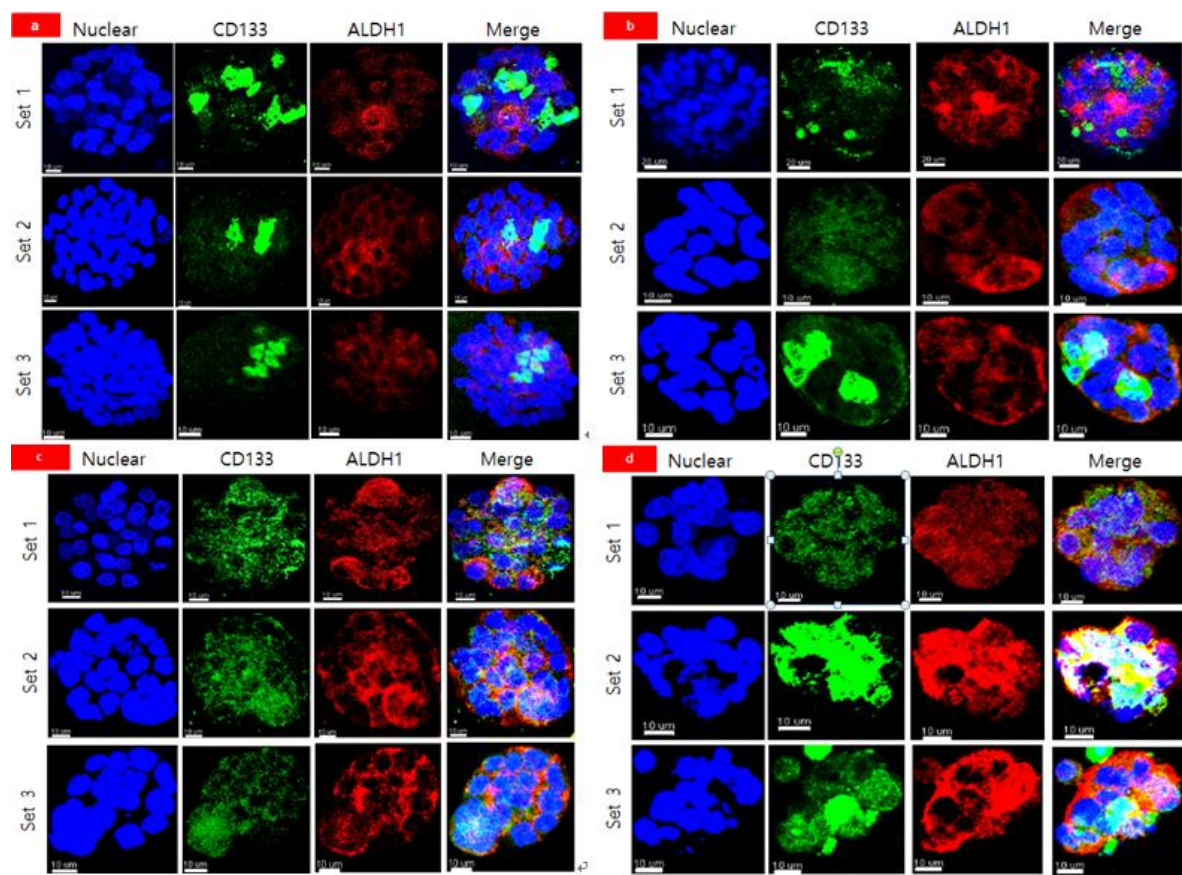
Figure 3. Representative confocal images of cell spheroids treated with Aflatoxin-B1 concentrations of (a) 0, (b) 1, (c) 2.5 and (d) 5 μM; (e) fluorescence intensity of obtained images.

Table 1. Fluorescence intensity of the obtained images

		CD133 intensity	Average	ALDH1 intensity	Average
Aflatoxin B1 0µM	set 1	16.75	**11.7**	12.71	**12.5**
	set 2	10.36		14.98	
	set 3	8.09		9.81	
Aflatoxin B1 1µM	set 1	10.74	**16.8**	23.43	**20.1**
	set 2	13.29		18.51	
	set 3	26.45		18.45	
Aflatoxin B1 2.5µM	set 1	22.51	**22.4**	21.3	**22**
	set 2	17.58		22.79	
	set 3	27.22		21.87	
Aflatoxin B1 5µM	set 1	19.03	**30.9**	28.96	**38.6**
	set 2	40.96		47.48	
	set 3	32.82		39.21	
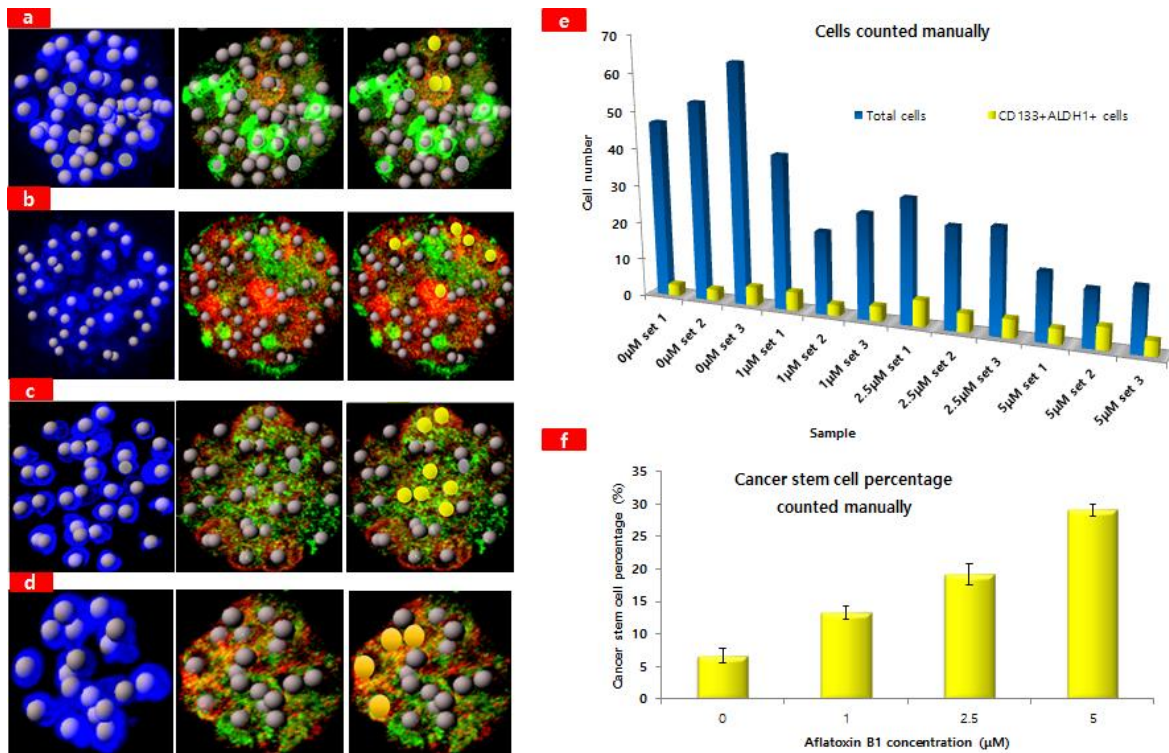
Figure 4. Representative images of spotted cancer stem cells (indicated by yellow dots) and non-cancer stem cells (indicated by grey dots) in HepG2 spheroid treated with Aflatoxin-B1 concentration of (a) 0, (b) 1, (c) 2.5, and (d) 5 μM; (e)Cell number counted manually from imaging data; (f) Mean cancer stem cells percentage counted manually from obtained images.

*Table 2. Number of cells counted manually from acquired imaging data*

		Total cells	CD133+ALDH1+ cells	%CSC	Average %CSC
Aflatoxin B1 0μM	set 1	47	3	6.4%	**6.63%**
	set 2	53	3	5.7%	
	set 3	64	5	7.8%	
Aflatoxin B1 1μM	set 1	41	5	12.2%	**13.33%**
	set 2	22	3	13.6%	
	set 3	28	4	14.2%	
Aflatoxin B1 2.5μM	set 1	33	7	21.2%	**19.19%**
	set 2	27	5	18.5%	
	set 3	28	5	17.9%	
Aflatoxin B1 5μM	set 1	18	4	22%	**29%**
	set 2	15	6	40%	
	set 3	17	4	23.5%	

3. Analysis of cancer stem cells by fluorescence-activated cell sorting (FACS)

To examine the hypothesis of cancer stem cells induction by Aflatoxin-B1, another method, FACS analysis is employed. Since cells after a 7-day growth exist as spheroid, where cells are attached to each other, collagenase NB 4G is utilized to disintegrate them into single cells so that flow cytometric analysis becomes possible. Figure 4 displays the result of FACS analysis result for 10000 cells disintegrated from HepG2 spheroids treated with the same aforementioned concentration range. In each graph, horizontal axis indicates ALDH1 emission, and vertical axis indicates CD133 emission. Based on fluorescence intensity, cells are divided into 4 types, corresponding to 4 quarters on the graphs. The upper-right quarter represents CD133-and-ALDH1 double positive cells, which are cancer stem cells defined by this study. It is evident that the percentage of cancer stem

cells increases as a function of concentration. In particular, at the control, cancer stem cells also exist, which account for around 6% of the whole population. Regarding treated samples, cancer stem cell population doubles to 12.4% at 1 µM, and it increases moderately to 15% at 2.5 µM. In addition, similarly to confocal imaging analysis, the highest cancer stem cell proportion was also detected at 5 µM sample, with 20.3%. This result has demonstrated a consistent pattern to the result of confocal imaging data, suggesting that the hypothesis about the impacts of Aflatoxin-B1 on cancer stem cell induction can be confirmed.
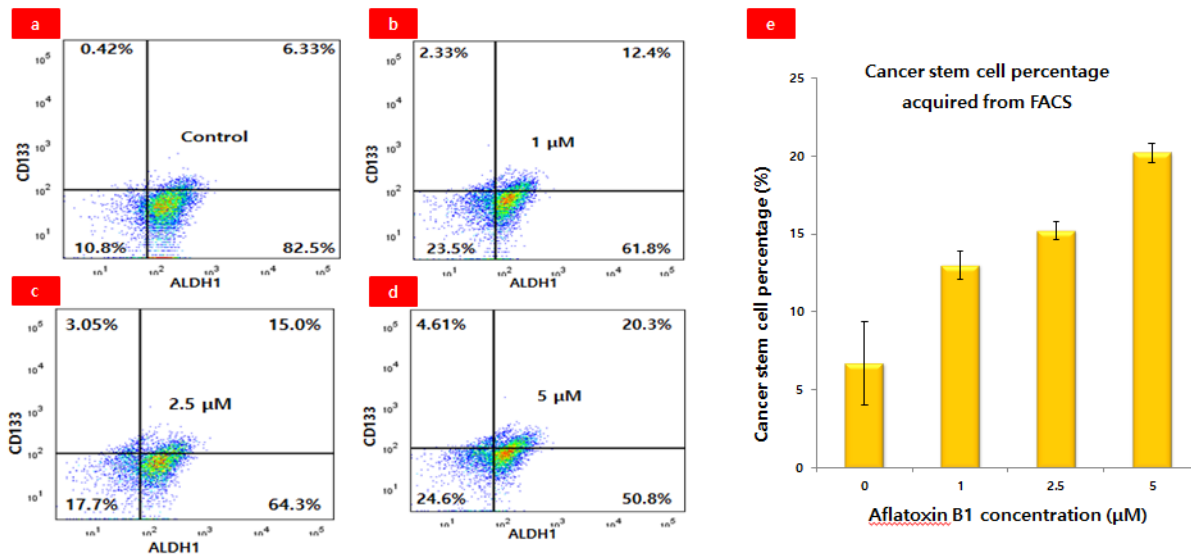
Figure 5. Representative FACS detection of cancer stem cells from HepG2 spheroid treated with Aflatoxin-B1 concentration of (a) 0, (b) 1, (c) 2.5, and (d) 5µM; (e) Cancer stem cell percentages of samples at 4 concentrations acquired from FACS analysis.

IV. DISCUSSION

Cancer has been a heated topic puzzling medical research for decades. Among various cancer types, it is estimated that in 2020, liver cancer accounted for 4.7% of total global new cancer cases, and became the third most lethargic cancer type, with 8.9% of total deaths (22). In addition, its treatment has been more demanding and posed challenge to current therapeutic strategies due to resistance and relapse and such problems have been mainly attributed to cancer stem cells (23). So far, cancer stem cell is defined by its clinical relevance and roles in cancer pathogenesis, rather than their biological characteristics (1). Therefore, there is no fixed standard in terms of which surface markers must be expressed in a cancer stem cells, leading to a difference in how different studies determine whether a cell population with a certain marker can be called cancer stem cell or not. For example, Sinh Truong Nguyen et al. (24) utilised HepG2 cells and employed only CD133 marker as the indicator for CSC isolation. Meanwhile, the present study selects CD133 and ALDH1 markers as the indication for sorting cancer stem cells because of their significant roles in displaying stem-like features. While CD133 involves a number of pathways related to drug resistance (25), (26), ALDH1 is critical in oxidising intracellular aldehydes (27) and facilitates cell proliferation (28). The relative amount of around 6%, reflected by analysis using both confocal imaging and flow cytometry, suggested that this selection is quite appropriate to proposed hypothesis of cancer stem cells, which states that they are a rare population in tumours.

Meanwhile, aflatoxin-B1 has been widely recognised as a carcinogen. However, its role as a cancer stem cell inducer has not been thoroughly investigated. Kawasaki et al. (29) isolated hepatoma K2 cells from rat exposed to aflatoxin-B1,

and found that 89% of cell population was occupied by cancer stem cells, while stemness genes such as *sox2, nanog* and *klf4* were also remarkably expressed. In addition, by treating HepG2 cells with various Aflatoxin-B1 concentrations and sorting out cancer stem cells based on surface marker, Hee Ju et al. (11) confirmed a similar result about aflatoxin-B1's ability to induce cancer stem cells. Nonetheless, both aforementioned findings were observed on 2D cell culture, which has been proved to have numerous limitations, making it findings less clinically significant. This study, which examines the phenomena on 3D cell culture, may offer a novel and more remarkable insight about actual effects of Aflatoxin-B1 on cancer stem cell formation in a tumour.

In this study, two methods were employed to determine the existence of cancer stem cells. Regarding confocal imaging, analysis on single cell level indicates that the higher Aflatoxin-B1 concentration is treated, the lower cell number a spheroid has. This can be attributed by the dual influence exerted by aflatoxin-B1. Specifically, while Aflatoxin-B1 reportedly induces cancer stem cells, it also causes DNA damage, and the phenomenon becomes more obvious at high concentration (30). This also explains a deviation between the results obtained from two methods. In fact, in the aforementioned result, similarities can be seen in the control and low dose-treated samples, but when Aflatoxin-B1 concentration was elevated, differences in cancer stem cell level acquired by flow cytometry and confocal imaging became more tangible. Indeed, as spheroids in high dose-treated sample have fewer cells, each single cell accounted for a bigger percentage to the total population. Hence, an absolute change of 1 cancer stem cells counted manually results in a more significant deviation in the relative proportion. Also, due to inhibitive effects of Aflatoxin-B1, it is also observed that there are more single cells fixed in gel, which cannot be distinguished and excluded in flow

cytometry analysis, although they can contributes to the result, regardless of which markers they express. However, with the percentages range from 6% to around 30% in both methods, and an increase in the cancer stem cell rate as higher dose is treated, the hypothesis of whether Aflatoxin-B1 induces cancer stem cells in 3D cell culture models has been confirmed; on the other hand, the similarity between 2 methods also proves that the developed 3D culture models, as well as confocal imaging analysis offer an applicable approach to study cancer stem cells, which has been examined by the casual methods of flow cytometry.

Since an increase in cancer stem cell level is reflected by an increase frequency of CD133 and ALDH1 found in the sample, its mechanism may be closely related to the expression of these two markers. In fact, it has been widely recognised that once metabolised, Aflatoxin-B1's metabolite of exo-Aflatoxin B1-8,9-epoxide can lead to various mutations on p53 protein, among which the one at third base codon 249 is the most significant in cancer pathogenesis (31). So far, there have been rising findings indicating that this mutation serves as a means by which insulin-like growth factor 2 (IGF-2) becomes over-expressed (32). While Xu et al. (33) have demonstrated a positive correlation between IGF-2 and CD133 expression in esophageal squameous cell carcinoma, similar link can be expected in liver cancer.

V. CONCLUSION

The present study has developed a 3D cell culture model to monitor cancer stem cell formation under the effect of Aflatoxin-B1. Induced cancer stem cells are observed using 2 distinct methods, confocal imaging and fluorescence-activated cell sorting. In both methods, the correlation between Aflatoxin-B1 dose and cancer stem cell level can be observed, in which the higher concentration was treated, the more cancer stem cells were detected. The similarity between detailed results of two methods suggests that the 3D cell culture model has been successfully established to study the capability of Aflatoxin-B1 to induce cancer stem cells.

VI. REFERENCE

1.   Yu Z, Pestell TG, Lisanti MP, Pestell RG. Cancer Stem Cells. Int J Biochem Cell Biol. 2012 Dec;44(12):2144–51.

2.   Schulz A, Meyer F, Dubrovska A, Borgmann K. Cancer Stem Cells and Radioresistance: DNA Repair and Beyond. Cancers. 2019 Jun 21;11(6):862.

3.   Pagotto A, Pilotto G, Mazzoldi EL, Nicoletto MO, Frezzini S, Pastò A, et al. Autophagy inhibition reduces chemoresistance and tumorigenic potential of human ovarian cancer stem cells. Cell Death Dis. 2017 Jul;8(7):e2943–e2943.

4.   Wei MF, Chen MW, Chen KC, Lou PJ, Lin SYF, Hung SC, et al. Autophagy promotes resistance to photodynamic therapy-induced apoptosis selectively in colorectal cancer stem-like cells. Autophagy. 2014 Jul 29;10(7):1179–92.

5.   Basuli D, Tesfay L, Deng Z, Paul B, Yamamoto Y, Ning G, et al. Iron addiction: a novel therapeutic target in ovarian cancer. Oncogene. 2017 Jul;36(29):4089–99.

6.   Lapidot T, Sirard C, Vormoor J, Murdoch B, Hoang T, Caceres-Cortes J, et al. A cell initiating human acute myeloid leukaemia after transplantation into SCID mice. Nature. 1994 Feb;367(6464):645–8.

7.   Masciale V, Grisendi G, Banchelli F, D'Amico R, Maiorana A, Sighinolfi P, et al. Isolation and Identification of Cancer Stem-Like Cells in Adenocarcinoma and Squamous Cell Carcinoma of the Lung: A Pilot Study. Front Oncol [Internet]. 2019 [cited 2023 Feb 4];9. Available from: https://www.frontiersin.org/articles/10.3389/fonc.2019.01394

8.   Suetsugu A, Nagaki M, Aoki H, Motohashi T, Kunisada T, Moriwaki H. Characterization of CD133+ hepatocellular carcinoma cells as cancer stem/progenitor cells. Biochem Biophys Res Commun. 2006 Dec 29;351(4):820–4.

9.   Fu JJ, Zhou Y, Shi XX, Kang YJ, Lu ZS, Li Y, et al. Spontaneous formation of tumor spheroid on a hydrophilic filter paper for cancer stem cell enrichment. Colloids Surf B Biointerfaces. 2019 Feb 1;174:426–34.

10.   Verma RJ. Aflatoxin Cause DNA Damage. Int J Hum Genet. 2004 Dec 1;4(4):231–6.

11.   Ju H, Shim Y, Arumugam P, Song JM. Crosstalk-eliminated quantitative determination of aflatoxin B1-induced hepatocellular cancer stem cells based on concurrent monitoring of CD133, CD44, and aldehyde dehydrogenase1. Toxicol Lett. 2016 Jan 22;243:31–9.

12.   Birgersdotter A, Sandberg R, Ernberg I. Gene expression perturbation in vitro—A growing case for three-dimensional (3D) culture systems. Semin Cancer Biol. 2005 Oct 1;15(5):405–12.

13.   Yip D, Cho CH. A multicellular 3D heterospheroid model of liver tumor and stromal cells in collagen gel for anti-cancer drug testing. Biochem Biophys Res Commun. 2013 Apr 12;433(3):327–32.

14.   Antoni D, Burckel H, Josset E, Noel G. Three-Dimensional Cell Culture: A Breakthrough in Vivo. Int J Mol Sci. 2015 Mar;16(3):5517–27.

15.   Bokhari M, Carnachan RJ, Cameron NR, Przyborski SA. Culture of HepG2 liver cells on three dimensional polystyrene scaffolds enhances cell structure and function during toxicological challenge. J Anat. 2007;211(4):567–76.

16.   Schyschka L, Sánchez JJM, Wang Z, Burkhardt B, Müller-Vieira U, Zeilinger K, et al. Hepatic 3D cultures but not 2D cultures preserve specific transporter activity for acetaminophen-induced hepatotoxicity. Arch Toxicol. 2013 Aug 1;87(8):1581–93.

17.   Langhans SA. Three-Dimensional in Vitro Cell Culture Models in Drug Discovery and Drug Repositioning. Front Pharmacol [Internet]. 2018 [cited 2023 Feb 4];9. Available from: https://www.frontiersin.org/articles/10.3389/fphar.2018.00006

18.   Ding W, Mouzaki M, You H, Laird JC, Mato J, Lu SC, et al. CD133+ Liver Cancer Stem Cells from Methionine Adenosyl Transferase 1A–Deficient Mice Demonstrate Resistance to Transforming Growth Factor (TGF)-β–Induced Apoptosis. Hepatol Baltim Md. 2009 Apr;49(4):1277–86.

19.   Rountree CB, Ding W, He L, Stiles B. Expansion of CD133-Expressing Liver Cancer Stem Cells in Liver-Specific Phosphatase and Tensin Homolog Deleted on Chromosome 10-Deleted Mice. Stem Cells Dayt Ohio. 2009 Feb;27(2):290–9.

20.   Lan X, Wu YZ, Wang Y, Wu FR, Zang CB, Tang C, et al. CD133 silencing inhibits stemness properties and enhances chemoradiosensitivity in CD133-positive liver cancer stem cells. Int J Mol Med. 2013 Feb 1;31(2):315–24.

21.   Clark DW, Palle K. Aldehyde dehydrogenases in cancer stem cells: potential as therapeutic targets. Ann Transl Med. 2016 Dec;4(24):518.

22.   Sung H, Ferlay J, Siegel RL, Laversanne M, Soerjomataram I, Jemal A, et al. Global Cancer Statistics 2020: GLOBOCAN Estimates of Incidence and Mortality Worldwide for 36 Cancers in 185 Countries. CA Cancer J Clin. 2021;71(3):209–49.

23.   Zhou HM, Zhang JG, Zhang X, Li Q. Targeting cancer stem cells for reversing therapy resistance: mechanism, signaling, and prospective agents. Signal Transduct Target Ther. 2021 Feb 15;6(1):1–17.

24.   Nguyen ST, Nguyen LS, Nguyen THP, Vo PH, Do NM, Truong KD, et al. Isolation of cancer stem-like cells from hepatocellular carcinoma cell line HepG2 by methods of magnetic-activated cell sorting, spheroid culture, and anti-tumor drug-resistant selection: A primary evaluation. Prog Stem Cell. 2020 Mar 18;7(1–2):279–89.

25.   Inhibition of CD133 Overcomes Cisplatin Resistance Through Inhibiting PI3K/AKT/mTOR Signaling Pathway and Autophagy in CD133-Positive Gastric Cancer Cells - Ruiqi Lu, Gang Zhao, Yulong Yang, Zhaoyan Jiang, Jingli Cai, Hai Hu, 2019

26.   Zhou L, Sun Y, Ye G, Zhao Y, Wu J. Effects of CD133 expression on chemotherapy and drug sensitivity of adenoid cystic carcinoma. Mol Med Rep. 2022 Jan 1;25(1):1–11.

27.   Tomita H, Kanayama T, Niwa A, Noguchi K, Ishida K, Niwa M, et al. Cancer Stem Cells and Aldehyde Dehydrogenase 1 in Liver Cancers [Internet].

Updates in Liver Cancer. IntechOpen; 2017 [cited 2023 Feb 4]. Available from: https://www.intechopen.com/chapters/53120

28.   Wei Y, Li Y, Chen Y, Liu P, Huang S, Zhang Y, et al. ALDH1: A potential therapeutic target for cancer stem cells in solid tumors. Front Oncol [Internet]. 2022   [cited   2023   Feb   4];12.   Available   from: https://www.frontiersin.org/articles/10.3389/fonc.2022.1026278

29.   Kawasaki Y, Adachi N, Yamazaki T, Todoroki R, Gotou Y, Komiya Y, et al. Cancer stem cells in aflatoxin B1-induced rat hepatocellular carcinoma K2 cells. Mycotoxins. 2007;57(2):87–93.

30.   Feng WH, Xue KS, Tang L, Williams PL, Wang JS. Aflatoxin B1-Induced Developmental and DNA Damage in Caenorhabditis elegans. Toxins. 2016 Dec 26;9(1):9.

31.   Link T, Iwakuma T. Roles of p53 in extrinsic factor-induced liver carcinogenesis. Hepatoma Res. 2017;3:95–104.

32.   Lee YI, Lee S, Das GC, Park US, Park SM, Lee YI. Activation of the insulin-like growth factor II transcription by aflatoxin B1 induced p53 mutant 249 is caused by activation of transcription complexes; implications for a gain-of-function during the formation of hepatocellular carcinoma. Oncogene. 2000 Aug;19(33):3717–26.

33.   Xu WW, Li B, Zhao JF, Yang JG, Li JQ, Tsao SW, et al. IGF2 induces CD133 expression in esophageal cancer cells to promote cancer stemness. Cancer Lett. 2018 Jul 1;425:88–100.

국문 초록

3D 바이오프린팅을 이용한

Aflatoxin B1-유도 암 줄기세포의 측정

Aspergillus flavus 와 *Aspergillus parasiticus* 라는 곰팡이 종에서 유래된 곰팡이 독소인 Aflatoxin B1 은 발암성으로 널리 알려져 있다. 그러나 암 줄기세포 유도에 대한 영향은 여전히 모호하며, 이것은 오직 2D 세포 배양 모델에서만 관찰되었다. 그러나 2D 세포 배양의 한계와 *in vivo* 환경과의 차이 때문에 임상적으로 더욱 관련성 있는 관찰이 이루어져야 한다. 본 연구는 Aflatoxin B1 노출이 HepG2 간암 세포주에서 암 줄기세포 수를 증가시키는지에 대한 가설을 검증하기 위해 3D 바이오프린팅을 이용한 세포 배양을 개발한다. 7 일간의 spheroid 배양과 48 시간의 Aflatoxin-B1 처리 후, 두 개의 바이오마커인 CD133 또는 prominin-1 과 Aldehyde dehydrogenase 1(ALDH1)을 사용하여 암 줄기세포를 spheroid 로부터 분리한다. 여기서 spheroid 를 아래의 두 가지 방법을 사용하여 분석한다. 공초점 이미징은 두 마커의 가시성을 보여주지만 형광 활성화 세포 분류(FACS)는 전체 세포 수에서 차지하는 암 줄기세포의 비율에 대한 정량적 결과를 제공한다. 두 방법의 결과는 Aflatoxin-B1 농도가 증가했을 때 암 줄기세포 비율이 증가함을 보여준다. 한편, 하나 이상의 방법으로 얻은 증가는 Aflatoxin-B1 노출과 암 줄기세포 형성 사이의 상관관계를 강조합니다. 반면에, 두 분석 방법 사이의 유사성은 flow cytometry 와 관련된 일반적인 기술 외에도 공초점 이미징이 종양의 자연적 형태를 방해하지 않으면서 암 줄기 세포 분석에 대한 신뢰할 수 있는 발견을 제공할 수 있다고 제안했다.